

# Impact of Recombinant Human Bone Morphogenetic Protein-2 on Residual Ridge Resorption After Tooth Extraction: An Experimental Study in the Rat

Khairul Matin, BDS, PhD<sup>1</sup>/Hiroaki Nakamura, DDS, PhD<sup>2</sup>/Kazuharu Irie, DDS, PhD<sup>3</sup>/  
Hidehiro Ozawa, DDS, PhD<sup>4</sup>/Sadakazu Ejiri, DDS, PhD<sup>5</sup>

*Residual ridge resorption begins following tooth extraction and continuously reduces alveolar bone volume, potentially creating a significant problem in dental implant treatment. In this study, the role of recombinant human bone morphogenetic protein-2 (rhBMP-2) in residual ridge resorption after tooth extraction was investigated. A polylactic acid/polyglycolic acid copolymer-coated gelatin sponge carrier was implanted with or without rhBMP-2 (1 µg) in the mesial root sockets after removal of maxillary first molars in male Wistar rats. Fine structural and histomorphologic analyses were conducted 3 to 84 days after implantation. Direct bone formation was first observed after 5 days on the rhBMP-2 side, which was transformed into cortical alveolar ridge with a smooth periosteal layer by 84 days, whereas the control side displayed slower healing. Bone histomorphometry revealed greater total bone area and increased bone height after 14, 28, 56, and 84 days on the rhBMP-2 side compared to the control side, and differences were significant after 14, 28, and 56 days. Larger numbers of proliferating cells and densely populated differentiating mesenchymal cells were observed on the rhBMP-2 side than on the control side in the early stage, and chondrogenesis was not observed. The findings indicate that rhBMP-2 may stimulate proliferation and differentiation of mesenchymal cells in the rat maxillary root socket to preserve cortical bone volume in the socket without any evidence of chondrogenesis. (INT J ORAL MAXILLOFAC IMPLANTS 2001;16:400-411)*

**Key words:** absorbable gelatin sponge, alveolar bone, bone morphogenetic proteins, bone resorption

Resorption of alveolar bone that occurs following tooth extraction is termed *residual ridge resorption*. In humans, an average residual ridge resorption of 2 mm occurs during the first 2 months after

tooth extraction, with and/or without dentures, and a further 2 mm of resorption takes place by 1 year after tooth extraction with dentures.<sup>1</sup> Over the last 4 decades, numerous efforts have been made to either prevent residual ridge resorption or to regenerate alveolar bone mass. Various bone regeneration methods have been or are being investigated and clinically applied in both the dental and orthopedic fields. Methods include autografts, allografts, osteoinduction by cytokines or growth factors, osteopromotion by the guided bone regeneration (GBR) technique, osteopromotion by low-power laser, immediate placement of dental implants, and combinations of these.<sup>2-9</sup>

Recombinant human bone morphogenetic protein-2 (rhBMP-2) is a synthetic protein that has been widely tested for bone induction and regeneration. Previous reports have shown that this novel protein molecule induces bone formation at ectopic sites and trephine defects in animal models.<sup>10,11</sup> As a member of the transforming growth factor- $\beta$  (TGF- $\beta$ ) super

<sup>1</sup>Researcher, Former PhD Student, Department of Fixed Prosthetic Dentistry, Niigata University School of Dentistry, Niigata, Japan; Currently, Assistant Professor, Bangladesh Medical Studies and Research Institute, Dhaka, Bangladesh.

<sup>2</sup>Associate Professor, Department of Oral Anatomy, Okayama University School of Dentistry, Okayama, Japan.

<sup>3</sup>Lecturer, Department of Oral Anatomy, Health Sciences University of Hokkaido, Hokkaido, Japan.

<sup>4</sup>Director and Professor, Institute for Dental Science and Department of Oral Anatomy, Matsumoto Dental University, Shiojiri, Japan.

<sup>5</sup>Associate Professor, Department of Oral Anatomy, Niigata University School of Dentistry, Niigata, Japan.

**Reprint requests:** Prof Hidehiro Ozawa, Institute for Dental Science and Department of Oral Anatomy, Matsumoto Dental University, 1780 Gobara, Hirooka, Shiojiri, Nganano, Japan. Fax +81-263-51-2192.

family, rhBMP-2 has displayed its potential in differentiating mesenchymal precursors into cartilage, bone, and cementum-forming cells.<sup>12-14</sup> Demonstration of its effectiveness in regenerating alveolar bone and cementum by expanded polytetrafluoroethylene (e-PTFE) membrane and rhBMP-2 has also led to its use in alveolar bone regeneration.<sup>14</sup> However, reports of attempts at immediate alveolar bone regeneration following tooth extraction for prosthodontic rehabilitation purposes are limited.<sup>6,9,15</sup>

A simple, moldable, and effective carrier for rhBMP-2 for dental use remains to be identified. In this experiment, a polylactic acid and polyglycolic acid copolymer-coated gelatin sponge (PLGA/GS) was used as a carrier for rhBMP-2 to preserve alveolar bone volume after maxillary tooth extraction in the rat.

Bone morphogenetic proteins (BMPs) in general induce a complex cascade of chemotaxis, proliferation, and cellular differentiation that closely resembles the normal process of embryonic bone formation, including both intramembranous and endochondral bone.<sup>16</sup> Cartilage phenotype expression has been observed during intramembranous bone formation in the sockets of rats, and endochondral bone formation by rhBMP-2 has been observed in rat mandibular defects.<sup>17,18</sup> Therefore, it is of interest to confirm rhBMP-2 behavior during socket healing.

This experiment investigated the regeneration process with and without rhBMP-2 by fine structural, histologic, histomorphometric, and histochemical methods. The effect of rhBMP-2 on osteoblastic cell proliferation was examined immunohistochemically.

## MATERIALS AND METHODS

### Animals and Materials

The protocol for this animal experiment was approved by the Committee on Guidelines for Animal Experimentation of Niigata University School of Dentistry, Niigata, Japan. Six-week-old male Wistar rats (170 to 190 g, Charles River Laboratory, Yokohama, Japan) were housed under similar conditions (22°C room temperature, 40% humidity, and a 12-hour daylight cycle) and were fed commercial rat food (MF, Oriental Yeast, Tokyo, Japan) and tap water ad libitum.

A gelatin sponge (GS) (Yamanouchi Pharmaceutical Industries, Tokyo, Japan) coated with polylactic acid/polyglycolic acid copolymer (PLGA) was used as the rhBMP-2 carrier.<sup>19</sup> The molar ratio of PLGA polymers was 1:1, and the weight ratio of PLGA:GS was 4:1, with approximately 90% porosity.<sup>20</sup>

### Tooth Extraction and rhBMP-2 Administration

On the day of operation, buffer-diluted rhBMP-2 (40 µg/100 µL, Yamanouchi Pharmaceutical Industries; buffer contained L-glutamic acid, sodium chloride, glycine, glucose, and Tween 80) was infiltrated into the PLGA/GS and allowed to adsorb with the carrier for 30 minutes. The PLGA/GS was cut into pieces approximately 1.5 × 1.5 × 1.5 mm, each of which contained approximately 1 µg of rhBMP-2. Other pieces of PLGA/GS were soaked in buffer only and cut similarly into smaller pieces. The rats were anesthetized by diethyl ether inhalation followed by intraperitoneal (IP) administration of 0.5 mL/100 g body weight 8% chloral hydrate (Wako Pure Chemical Industries, Osaka, Japan). Then 2% xylocaine (Astra Japan, Osaka, Japan) was administered locally and the maxillary first molars were gently extracted. Buffer containing PLGA/GS was grafted into the upper part of the anterior root of 1 socket as control. The contralateral socket was similarly filled with the PLGA/GS containing rhBMP-2. Sockets were closed by suturing the gingiva.

### Tissue Processing

The rats were sacrificed at 3, 5, 7, 14, 21, 28, 56, and 84 days after the operation (8 rats/group, except for the 21-day group, which had only 4 rats; total n = 60). A total of 12 rats were injected with 5-bromodeoxyuridine (BrdU) (Sigma Chemical, St. Louis, MO) 1 hour before sacrifice at 3, 5, and 7 days after operation. They were anesthetized with a diethyl ether inhaler and intraperitoneal injection of 0.4 mL/kg body weight pentobarbital sodium (50 mg/mL, Abbott Laboratories, Abbott Park, IL) then perfused through the left ventricle with Ringer's solution and the fixatives as described below.

### Scanning Electron Microscopy

Fine structural analyses were performed by scanning electron microscopy (SEM) (Hitachi S-570, Tokyo, Japan). Rats were perfused with 2% paraformaldehyde and 2.5% glutaraldehyde in 0.05 mol/L cacodylate buffer solution, then immersed in the same fixative for 3 hours at 4°C. Soft tissues were removed by immersing the specimen in 5% sodium hypochlorite solution for 15 hours (the solution was changed at 3-hour intervals). Specimens were washed for 12 hours in distilled water and dehydrated in serially graded ethanol. They were then immersed in isoamyl acetate as the transitional fluid for about 10 minutes, which was replaced by carbon dioxide in a critical point-dryer (HCP-1, Hitachi); specimens were then gold-coated by an ion coater (IB-3, Eiko Engineering, Ibaraki, Japan). The maxillae were examined by SEM at 20 kV in a palatobuccal direction (Fig 1a).

## Histology

For histologic preparation, the rats were fixed with 4% paraformaldehyde and 0.5% glutaraldehyde in a 0.05 mol/L cacodylate buffer. Maxillae were dissected, decalcified in 10% EDTA-sodium solution for 20 days, dehydrated in serially graded alcohols, and embedded in paraffin. Serial sections of 5  $\mu$ m, cut through the mesial foramen (Fig 1a), were stained with hematoxylin-eosin (H&E).

## Bone Histomorphometry

Bone histomorphometry was performed at 14, 28, 56, 84 days after operation ( $n = 5$  for each group, except for controls at 14 days and both sides at 84 days, where  $n = 4$ ). H&E-stained serial sections cut through the mesial foramen (Fig 1a) were selected for the analysis. Photomicrographs were magnified 10 times with a profile projector (V-12, Nikon, Nippon Kagaku, Japan). As described by the diagram (Fig 1b), the total bone area (old bone + new bone), area of the carrier, bone marrow area, and other soft tissue areas inside the examined zone were traced on white paper and color-painted separately. With a cable camera, the traced images were digitized into a computerized image analyzer (IBAS 2000, Kontron M14, Munich, Germany). Binary image processing was performed in the computer to measure all above-mentioned areas and alveolar bone heights. Alveolar bone heights were calibrated by measuring the distance between the horizontal bars on vertical lines at points M, N, O, and P as described in Fig 1b. Means and standard deviations for all data were calculated by a personal computer. Data on respective items for rhBMP-2 groups and control groups were compared by paired Student *t* tests, and *P* values  $< .05$  were considered significant.

## Enzyme Histochemistry

Cryosections (16  $\mu$ m) from 3-, 5-, 7-, and 14-day specimens were obtained by a Minotome (Damon, Needham, MA); embedded with O.C.T. Compound (Tissue-Tek, Miles, Elkhart, IN); and used for detection of alkaline phosphatase (ALPase) activity. The sections were incubated according to the azo-dye method for 7 minutes at 37°C.

## Immunohistochemistry

Some paraffin sections from the BrdU-injected rats were used for immunohistochemical localization of BrdU by incubation with anti-BrdU monoclonal antibody (Mab anti-BrdU)<sup>21</sup> (Biodesign International, Kennebunk, ME) with methanol solution containing 0.3% hydrogen peroxide for 20 minutes at room temperature to block endogenous peroxidase. The sections were then incubated with 2 mol/L

hydrochloric acid for 30 minutes at 37°C to denatured DNA and neutralized with 0.1 mol/L sodium borate solution (pH 8.5) for 10 minutes. Nonspecific binding sites were blocked with 5% lowfat milk for 15 minutes at room temp. Sections were incubated with MAb anti-BrdU (dilution 1:500) overnight at 4°C. They were further incubated with biotinylated anti-mouse gamma G immunoglobulins (Histofine SAB-PO(M) kit, Nichirei Corporation, Tokyo, Japan) for 30 minutes, then with peroxidase-conjugated streptavidin (Histofine) for 15 minutes. Color was developed with a 3,3' diaminobenzidine (DAB) solution for 5 minutes at room temperature and counterstained with Goldner-Masson light green or eosin. They were photographed by a Vanox-S microscope (Olympus, Tokyo, Japan) at a magnification of  $\times 50$  in 2 locations per section (Fig 1c), and BrdU-positive cells were counted.

## RESULTS

### Effect on Gross Anatomy

The union of gingiva occurred at the mesial half of the whole socket within 7 days. The distal half remained open for about 14 days. From 14 to 28 days, a slight elevation could be recognized in the mesial root region on the rhBMP-2 side.

### Effect on Differentiation and Osteogenesis

At 5 days after surgery in the rhBMP-2 sockets, more densely populated ALPase-positive osteoblastic cells were observed throughout the socket than in the control sockets (Figs 2a and 2b). Some differentiating cells were present in the ridge area on the control side along the old bone, but there were fewer than on the rhBMP-2 side (Figs 2c and 2d). Formation of woven bone with densely populated ALPase-positive osteoblastic cells was marked at the mesial ridge area in rhBMP-2 sites (Fig 2d). No chondrogenesis could be detected during the above-mentioned histochemical studies either inside or outside the extraction socket.

### Effect on Bone Formation and Adaptation

Different paces and patterns were observed in socket healing between the control and rhBMP-2 groups. Clear and distinctive features could be recognized by SEM observation. Large cavities were seen in the control, indicating healing that was slower than in the rhBMP-2-treated sockets (Fig 3a). Dome-shaped new bone in the woven stage was observed at 28 days on the rhBMP-2 side (Fig 3b). At 56 days postsurgery, healing in the control side occurred slowly, with new bone yet to fill the socket

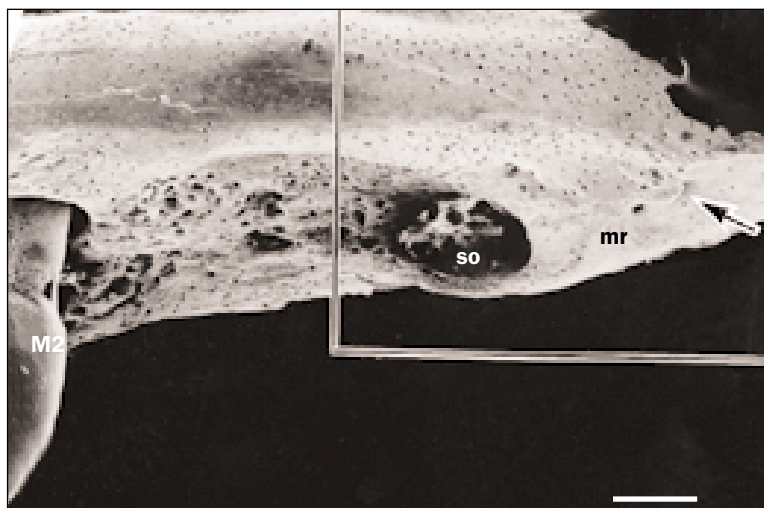


**Fig 1a** Scanning electron microscopy (SEM) of a rat maxilla; palatobuccal view showing extraction socket of the 1st molar. The mesial root socket is outlined by the square. The arrow indicates the mesial foramen through which sagittal paraffin sections were cut for bone histomorphometry. SO = socket; mr = mesial ridge; M2 = second molar; bar = 570  $\mu$ m.

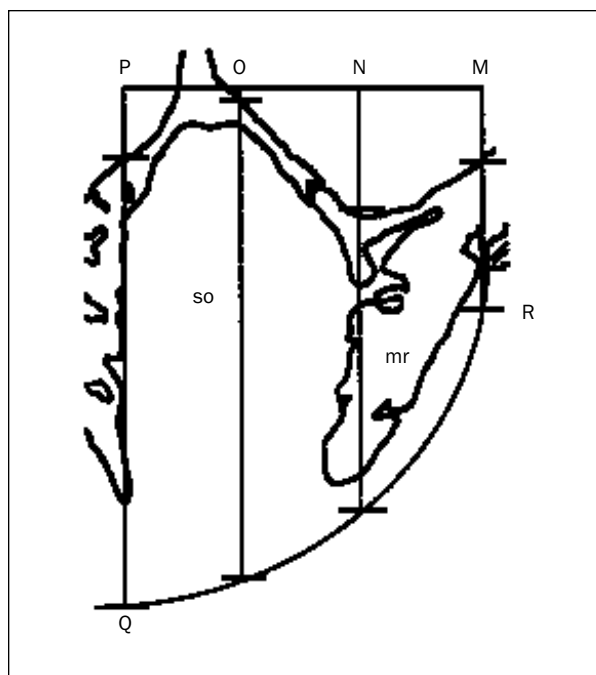


**Fig 1b** Diagrammatic representation of a paraffin section of the mesial root socket. Points M, P, Q, and R define the area selected for histomorphometric analysis. The M-R line was drawn medial to the mesial ridge, just distal to the muscle attachment and parallel to the mesial wall of the socket. A parallel line P-Q was drawn 1.8 mm distal to the M-R line, corresponding to the distal wall of the socket. The M-P line was drawn along the base of the socket. Q-R represents the oral border of the alveolar bone. Points M, N, O, and P were added by keeping an equal original distance of 0.6 mm, and alveolar bone height was measured between the horizontal bars on the lines that extend downward from these points.

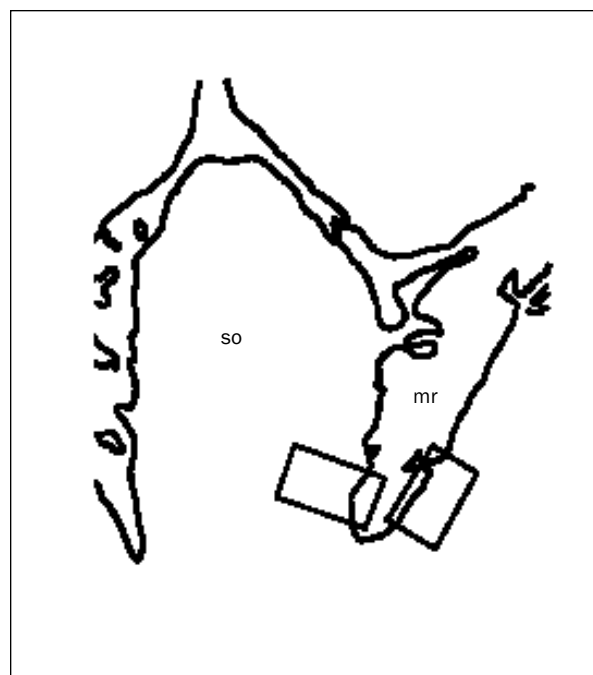
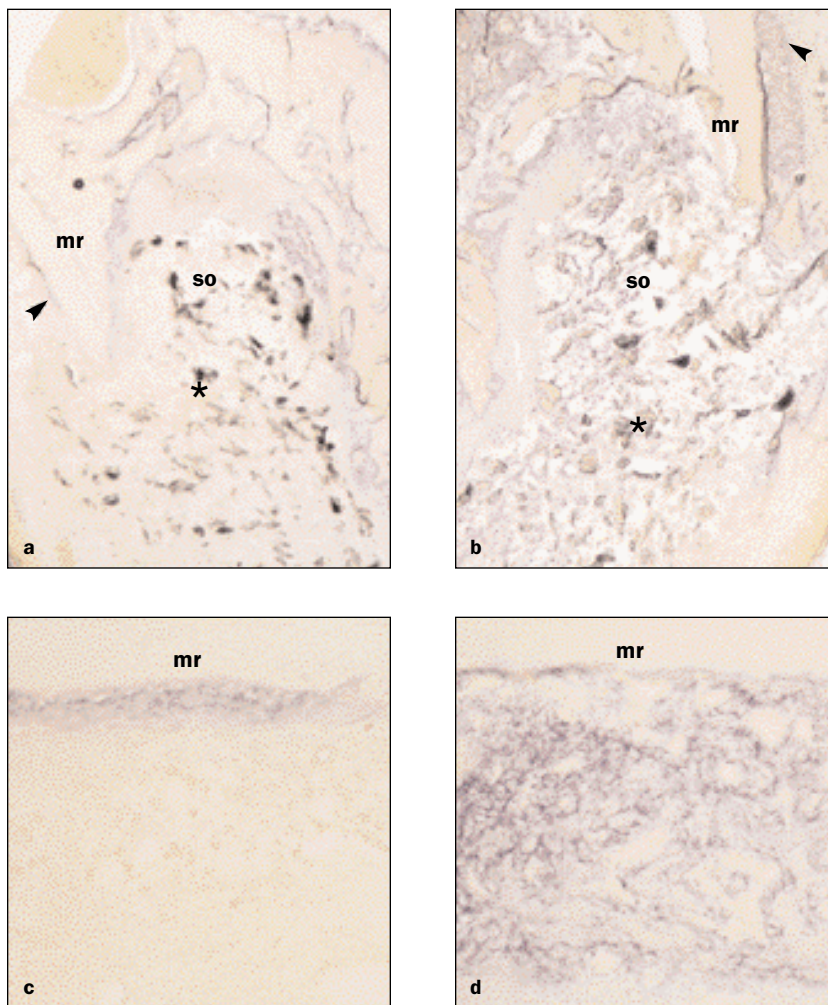


**Fig 1c** Diagram of same section. The squares show the locations selected for BrdU-positive cell count at an original magnification of  $\times 50$ .



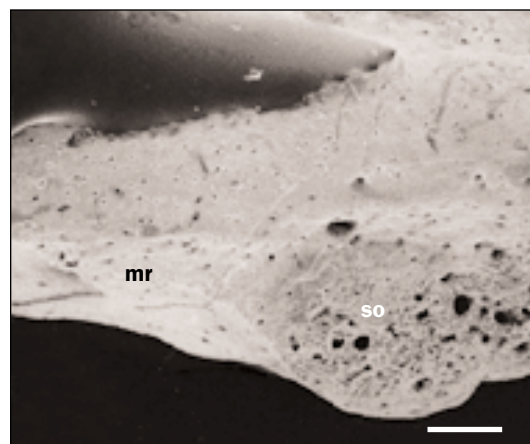
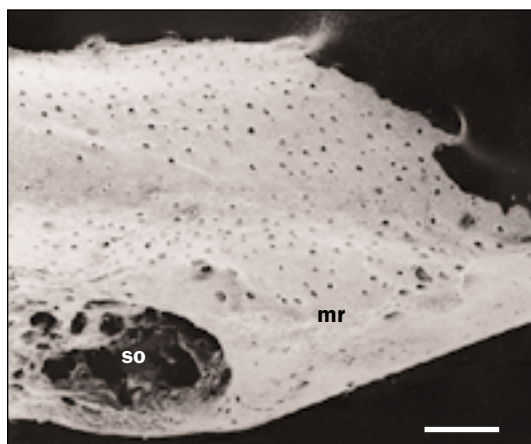
**Figs 2a to 2d** Localization of alkaline phosphatase (ALPase) activity. Figs 2a and 2c are control sites, and Figs 2b and 2d are rhBMP-2 sites. Figs 2a and 2b show the entire socket at low magnification ( $\times 10$ ), and Figs 2c and 2d show mesial ridges with newly formed woven bone (indicated by arrowheads in Figs 2a and 2b) at higher magnification ( $\times 50$ ). Densely populated ALPase-positive cells (deep blue stained) can be seen in and around the socket on the rhBMP-2 side, but only a very thin layer of ALPase-positive cells is apparent on the bone surface on the control side. mr = mesial ridge; SO = socket; asterisk = carrier; arrowhead = ALPase-positive cells.

(Fig 3c). In addition, there were some cavities left behind by unresorbed PLGA. The new bone induced by rhBMP-2 (Fig 3d) had lost some height since 28 days but still remained above the adjoining ridges. Excluding the small amount of woven bone at the center of the defect, the rest of the periosteal surface had become smooth and contained smaller osteocyte lacunae. At 84 days, the concavity at the opening of the socket on the control side was reduced further, but some small hollow defects remained at the center (Fig 3e), whereas on the rhBMP-2 side, new bone had remodeled to the adjoining ridge level with a comparatively smooth periosteal surface (Fig 3f). The ultrastructural features resembled the adjoining preexisting mature bone, containing small osteocyte lacunae.

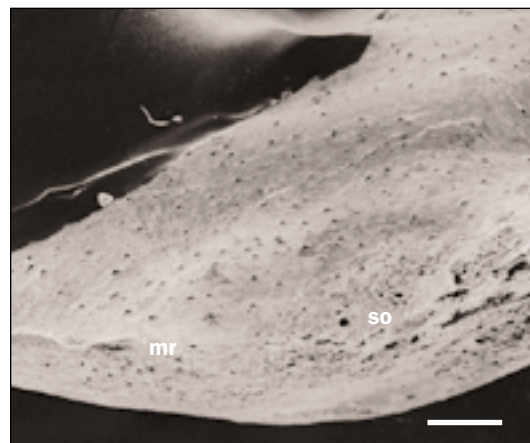
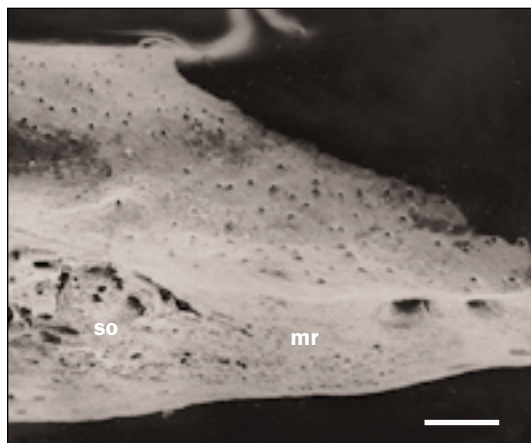
Histomorphometry (Fig 4a) showed that the total bone area (existing bone + new bone) was significantly greater in the rhBMP-2 group at 14, 28, and 56 days than in the control group (at all stages,  $P < .05$ ). At 84 days after operation, the total bone area was somewhat greater in the rhBMP-2 group than in the control group. There was a rapid increase in total bone area from 14 to 28 days in the rhBMP-2 group compared to the control group. Areas with the carrier shrank gradually and became nearly undetectable at 84 days on both sides (Fig 4b). At 56 days, areas with the carrier in the rhBMP-2 group were significantly ( $P < .05$ ) smaller than in the control group. Bone marrow within the measuring areas did not show significant differences, except at 56 days, when the rhBMP-2 group had a significantly greater bone marrow area ( $P$



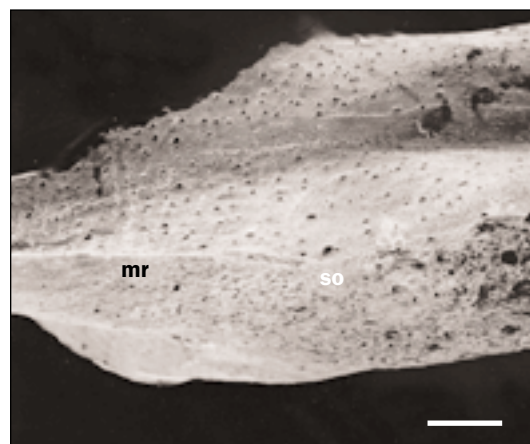
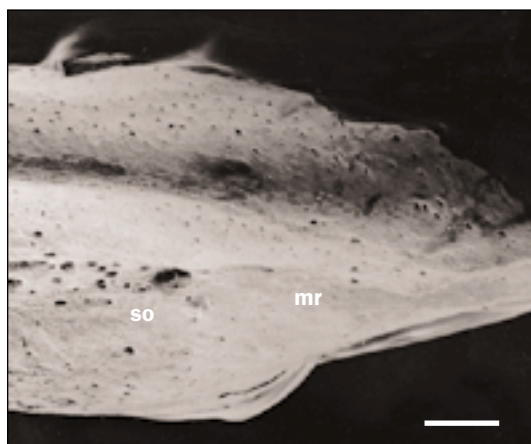
**Figs 3a to 3f** Scanning electron micrographs of the mesial root socket as shown by the square in Fig 1a. The figures at left are control sites, and the figures at right are rhBMP-2 sites.



**Figs 3a and 3b** Specimens at 28 days. (Left) A large cavity in the socket indicates delayed healing on the control side. (Right) Dome-shaped new bone formation is apparent at the opening of the socket in the rhBMP-2 side. Part of the dome, adjoining the ridges, appears to be transforming into compact form but otherwise looks spongy. mr = mesial ridge; SO = socket; bar = 340  $\mu$ m.



**Figs 3c and 3d** Specimens at 56 days. (Left) In the control side, socket healing occurred from the base, but a depression between the buccal and palatal ridge remains, and some small cavities are also seen at the opening of the socket. (Right) Convex-shaped new bone is transforming into compact bone entirely on the rhBMP-2 side. mr = mesial ridge; SO = socket; bar = 340  $\mu$ m.



**Figs 3e and 3f** Specimens at 84 days. The surface of the alveolar bone has become flat across the entire mesial root socket on the rhBMP-2 side (right), whereas the control side (left) remains concave with some small cavities. mr = mesial ridge; SO = socket; bar = 340  $\mu$ m.

**Figs 4a to 4d** Graphs representing histomorphometry at different time stages measured as described in Fig 1b (n = 4 for 14-day controls and 84 days in both groups; n = 5 for all other groups).

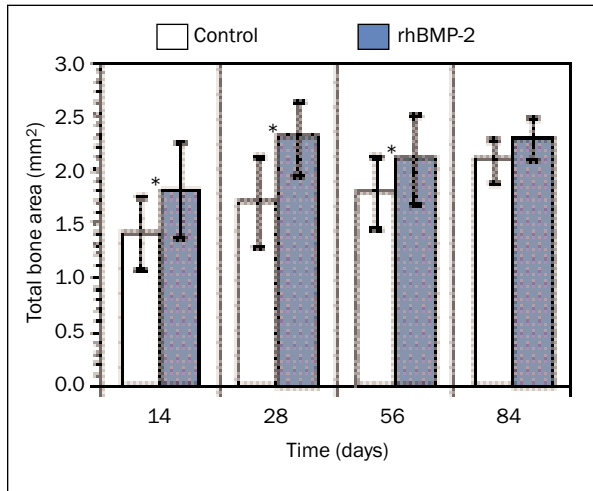


**Fig 4a** Total bone area. This was significantly greater in the rhBMP-2 group at 14, 28, and 56 days than in the control group. At 84 days, the rhBMP-2 side still had more bone, but bone area increased over time in both groups. \* $P < .05$ .

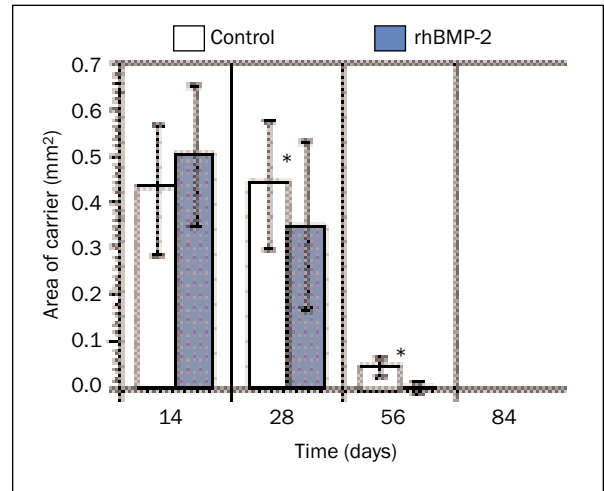


**Fig 4b** Area occupied by the carrier, which was gradually resorbed by 56 days in the rhBMP-2 group. \* $P < .05$ .

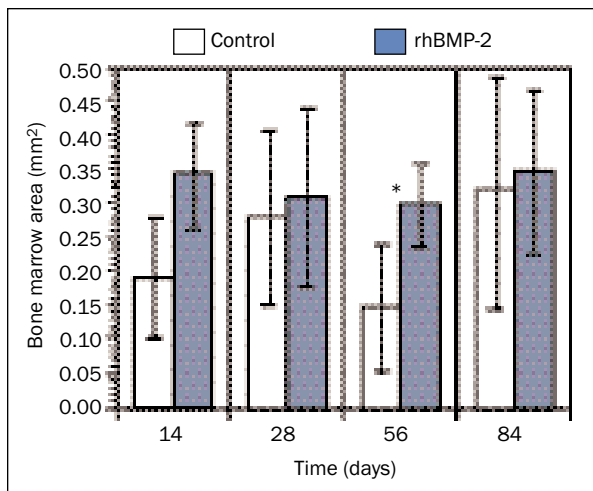


**Fig 4c** Bone marrow area. At 56 days bone marrow area in the control group was significantly smaller than in the rhBMP-2 group; otherwise, both groups maintained almost the same bone marrow area. \* $P < .05$ .

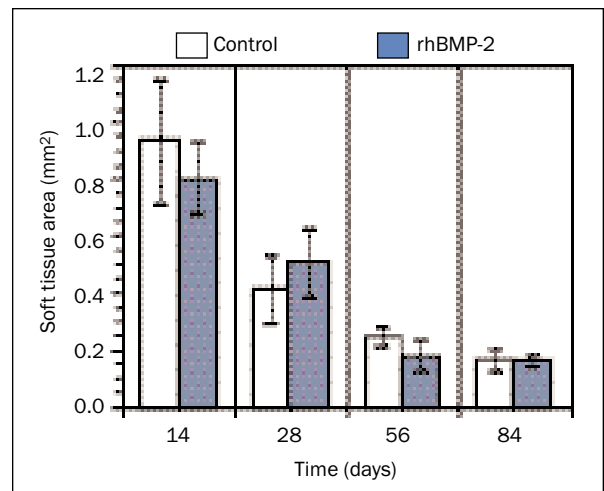


**Fig 4d** Soft tissue area other than bone marrow. This showed gradual reduction with time and became steady by 56 days in the rhBMP-2 group and by 84 days in the control group.

< .05) (Fig 4c). In the early stages, soft tissue areas were almost the same size in both the rhBMP-2 and control groups. The areas gradually shrank over time up to 56 days, and from this time they reached a steady state, particularly on the rhBMP-2 side (Fig 4d).

Alveolar bone heights (Figs 5a to 5d) were significantly greater in the rhBMP-2 group at 14, 28, and 56 days compared to the control group (at all times,  $P < .05$ ). Here also there was a rapid increase in alveolar bone height from 14 to 28 days in rhBMP-2 compared to the control. At 84 days postsurgery, slightly increased alveolar bone heights were detected in the rhBMP-2 side versus the control side (Fig 5d).

In the histologic examination, no major differences between the control and rhBMP-2 sides could be recognized in H&E-stained paraffin sections at 3 days after surgery (Figs 6a and 6b). Periodontal ligaments and fibroblasts were seen along the wall and at the bottom of the socket, and some inflammatory cells were also seen around the gelatin sponge. At 14 days, a small amount of new bone could be seen inside the socket on the control side (Fig 6c). New bone extended mostly toward the oral epithelium, and islands of new bone were formed between the carrier particles on the rhBMP-2 side (Fig 6d). Histologic examination at 84 days after surgery showed a

**Figs 5a to 5d** Graphs representing alveolar bone height measured at 4 points as described in Fig 1b.

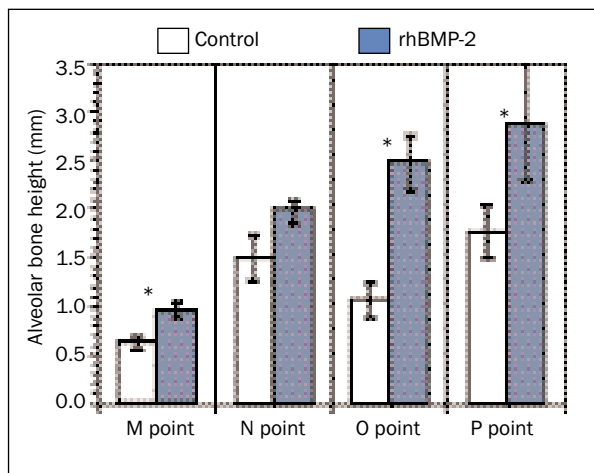


**Fig 5a** At 14 days, alveolar bone height was significantly increased in the rhBMP-2 group compared to controls at M point, O point, and P point (P point was the peak point, at 2.9 mm). \* $P < .05$ .

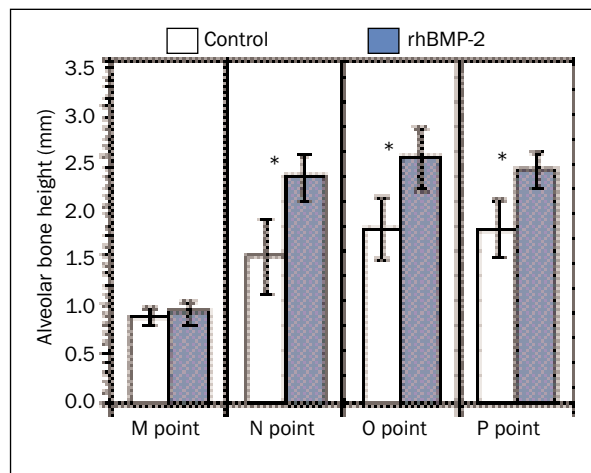


**Fig 5b** At 28 days, alveolar bone height remained significantly greater in the rhBMP-2 group than in the control group at N point, O point, and P point. The height had increased at the N point since 14 days, but it had decreased at O point and P point. \* $P < .05$ .

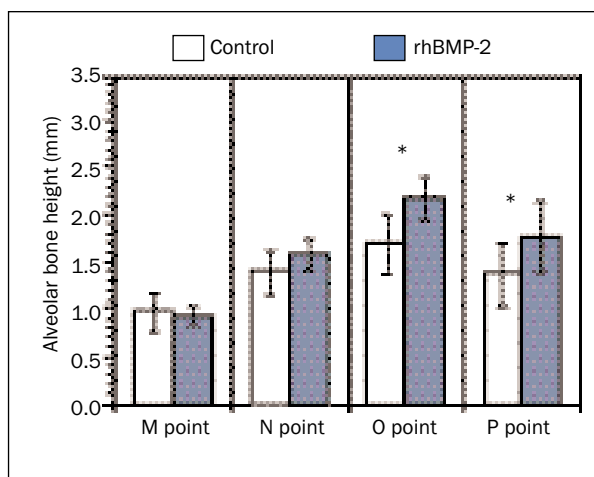


**Fig 5c** At 56 days, alveolar bone height was further reduced in rhBMP-2 group but still remained significantly greater at O point and P point. \* $P < .05$ .

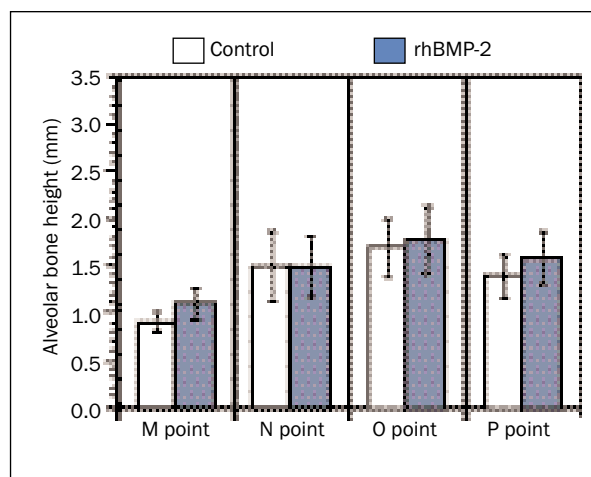


**Fig 5d** At 84 days, the difference in alveolar bone heights between the 2 groups was reduced.

rough periosteal surface and very small amounts of carrier particle on the control side (Fig 6e), while a smooth periosteal surface was observed on the rhBMP-2 side (Fig 6f). Thick cortical bone formed at the opening of the socket connecting the adjoining ridges on both sides, with a thicker layer forming in the rhBMP-2 side versus the control (Figs 6e and 6f).

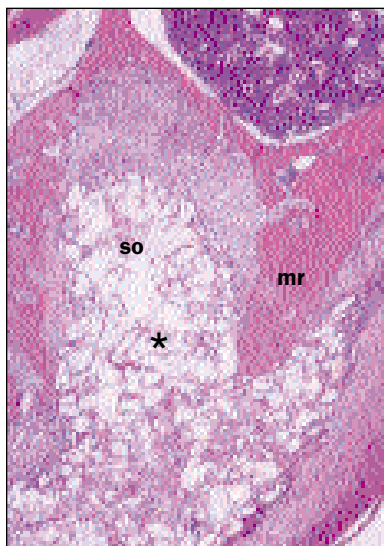
#### Effect on Proliferation

BrdU-positive immature mesenchymal cells were observed on the bone surface at the ridge area on both sides at 3 days (Figs 7a and 7b). More proliferating cells were detected on the rhBMP-2 side. At

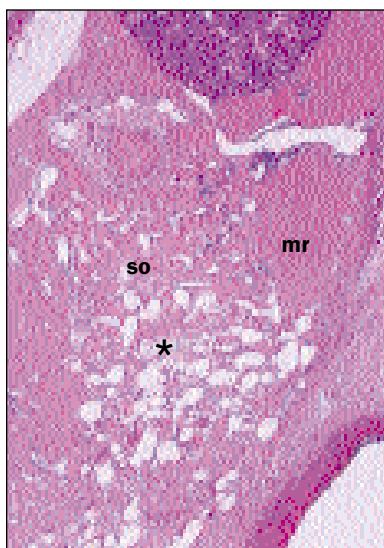
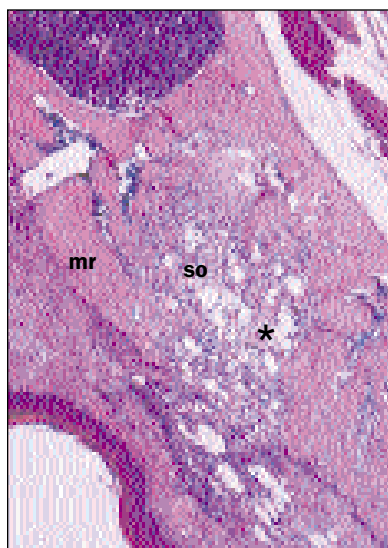
higher magnifications of the ridge area at 5 days, BrdU-positive mesenchymal cells on the control side (Fig 7a inset) and BrdU-positive osteoblast-like cells on the rhBMP-2 side (Fig 7b inset) were seen near the mesial ridge. Freshly deposited bone matrix was also seen around them on the rhBMP-2 side only. Both in the socket area (Figs 7c and 7d) and in the ridge area, there were significantly greater numbers ( $P < .001$ ) of BrdU-positive cells in the rhBMP-2 group compared to the control group at 5 days (Figs 8a and 8b). The greatest number of BrdU-positive cells was observed on the rhBMP-2 side at the ridge area at 5 days. Although proliferation was



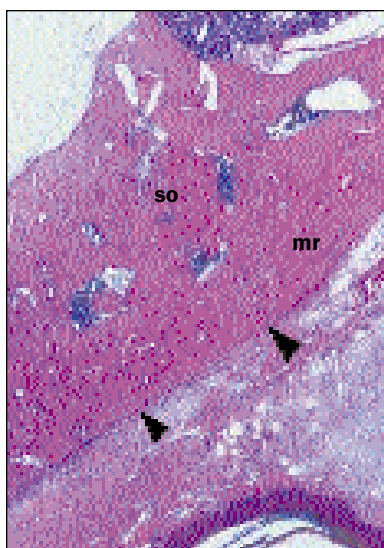
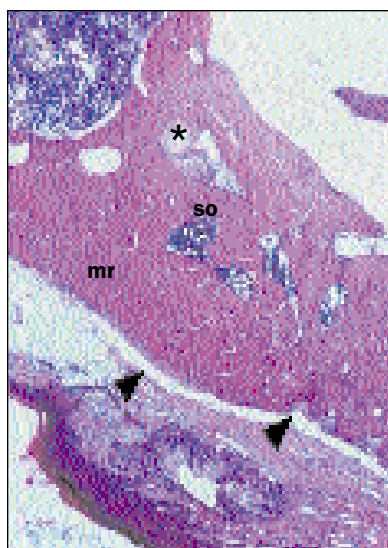
**Figs 6a to 6e** Hematoxylin and eosin (H&E) stained specimens viewed under light microscopy (×10).



**Figs 6a and 6b** (Left) Control specimen and (right) rhBMP-2 specimen at 3 days. There is no remarkable difference between the 2 groups. In both sides, cell infiltration inside the carrier particles is scant but appears to be condensing along border. mr = mesial ridge; SO = socket; asterisk = carrier.



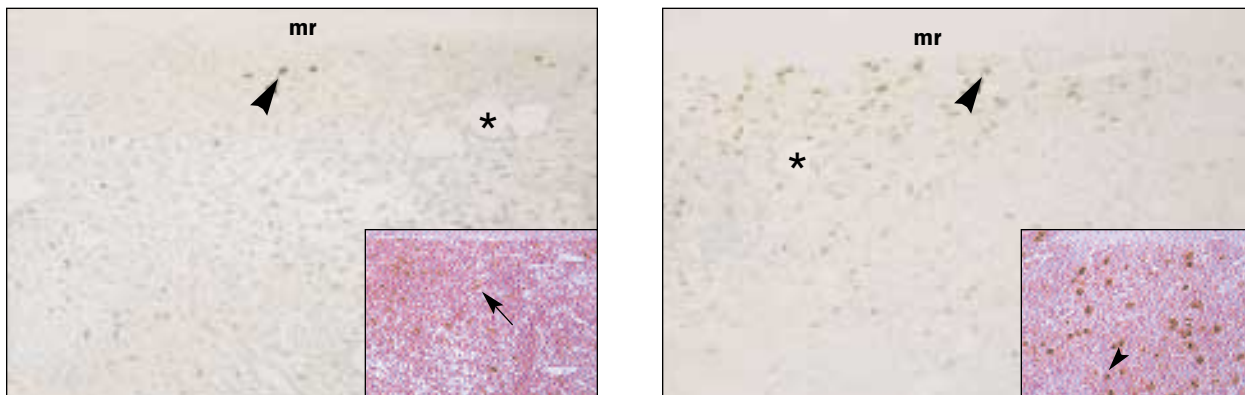
**Figs 6c and 6d** (Left) Control specimen and (right) rhBMP-2 specimen at 14 days. A small amount of new bone formation occurred inside the socket on the control side. On the rhBMP-2 side, new bone formation occurred inside the entire socket in between carrier particles and extended toward the oral epithelium. mr = mesial ridge; SO = socket; asterisk = carrier.



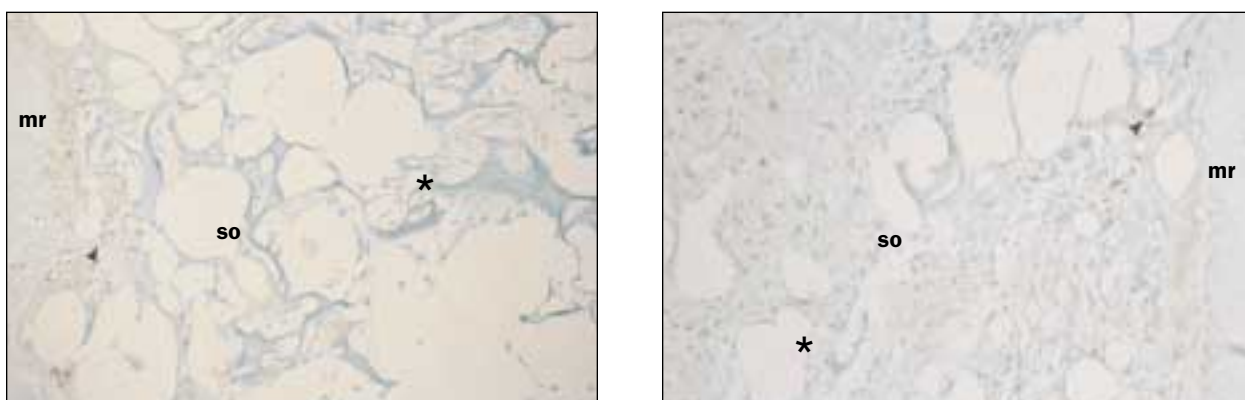
**Figs 6e and 6f** (Left) Control specimen and (right) rhBMP-2 specimen at 84 days. A small amount of connective tissue and some bone marrow spaces can be observed inside the matured bone on both sides. Very small amounts of carrier particles are visible on the control side, while a smooth periosteal surface can be seen on the rhBMP-2 side. A thick cortical layer is visible on both sides, with the rhBMP-2 side being the thicker of the two. mr = mesial ridge; SO = socket; asterisk = carrier; arrowheads = periosteal border of the new bone.

COPYRIGHT © 2001 BY QUINTESSENCE PUBLISHING CO., INC. PRINTING OF THIS DOCUMENT IS RESTRICTED TO PERSONAL USE ONLY. NO PART OF THIS ARTICLE MAY BE REPRODUCED OR TRANSMITTED IN ANY FORM WITHOUT WRITTEN PERMISSION FROM THE PUBLISHER.

**Figs 7a to 7d** Immunohistochemical localization of proliferating cells by 5-Bromo-2'-deoxyuridine (BrdU) monoclonal antibody.



**Figs 7a and 7b** (Left) Control specimen and (right) rhBMP-2 specimen at 3 days, showing BrdU-positive cells (nucleus stained brown) at the ridge area, with comparatively more on the rhBMP-2 side ( $\times 50$ ). Inset photomicrographs are higher magnifications ( $\times 400$ ) of ridge area at 5 days. BrdU-positive mesenchymal cells are seen near the mesial ridge on the control side. BrdU-positive osteoblast-like cells are seen near the ridge, along with freshly formed bone matrix (right, inset). mr = mesial ridge; SO = socket; asterisks = carrier; large arrowhead = BrdU-positive cells; arrow = mesenchymal cells; small arrowhead = osteoblast-like cells; ma = bone matrix.



**Figs 7c and 7d** (Left) Control specimen and (right) rhBMP-2 specimen showing BrdU-positive cells in the socket area at 5 days. Here also, BrdU-positive cells are more numerous on the rhBMP-2 side than on the control side. mr = mesial ridge; SO = socket; asterisk = carrier; arrowheads = BrdU-positive cells.

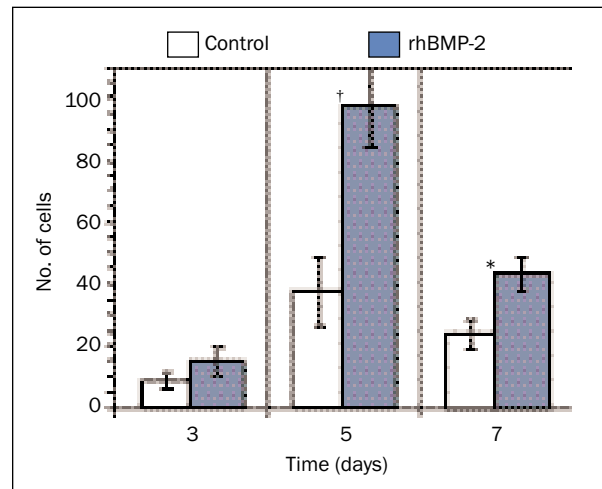
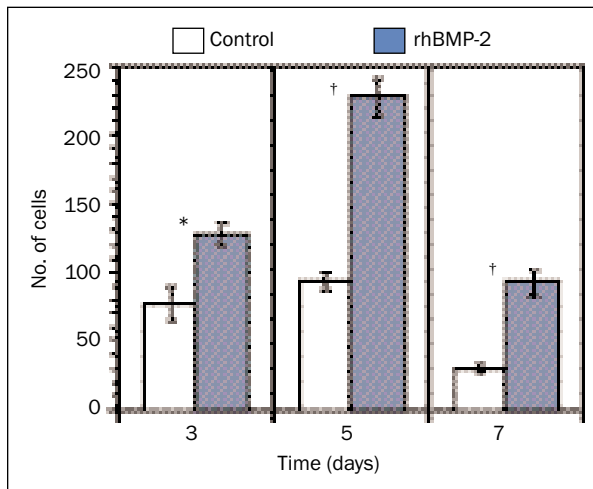
down-regulated at 7 days on both sides, the rhBMP-2 side had significantly greater numbers ( $P < .05$ ) of BrdU-positive cells (Figs 8a and 8b). Additionally, no cartilage formation could be detected during this proliferation stage. Chondrogenesis was not seen at any stage under H&E-stained light microscopy.

## DISCUSSION

Socket healing occurred in both the control and rhBMP-2 groups. In the control sites, healing occurred at a comparatively slower rate than in the rhBMP-2 sites. Sockets on the rhBMP-2 side healed from both inside the socket cavity and from the adjoining ridges (crest of the socket wall). In this experiment, bone formation was first recognized

outside the carrier on the mesial ridge at 5 days (Fig 2b). BrdU-positive and ALPase-positive cells were also recognized inside the carrier at the same stage. At 28 days, the new bone formed a dome at the ridge, which was transformed into cortical bone with a smoother periosteal surface by 84 days. Bone histomorphometry also showed that the total bone area and alveolar height were significantly greater in the rhBMP-2 group than in the control group up to 56 days. However, by 84 days, there were no significant differences in both parameters between the 2 groups. A smoother periosteal surface and smaller osteocyte lacunae indicated an increased maturation rate of woven bone in rhBMP-2 sites than in control sites.

Stimulatory effects of BMPs on osteoblastic cell proliferation have been observed in some in vitro experiments.<sup>22</sup> In contrast, one in vitro experiment



**Figs 8a and 8b** Graphs representing the number of BrdU-positive cells ( $n = 4$ ) in (left) the mesial ridge area and (right) the socket area, showing that the rhBMP-2 side always had more proliferating cells than the control side. There is also a peak at 5 days on the rhBMP-2 side, which had significantly more BrdU-positive cells than the control. \* $P < .05$ ; † $P < .001$ .

reported that rhBMP-2 stimulated proliferation of ROB-C26 (rat calvarial premature osteoblast-like cell) but inhibited proliferation of ROB-C20 (rat calvarial more differentiated calvarial osteoblastic cell).<sup>23</sup> The effects of BMPs on osteoblastic cell proliferation remain controversial. This present experiment clearly demonstrated that in vivo, the number of BrdU-positive proliferating cells was significantly greater in the rhBMP-2 sites than in the control sites. The level of DNA synthesis reached a peak at 5 days, which is much earlier than that of an osteoblast phenotype demonstrated in an in vitro experiment.<sup>24</sup> Proliferation was also significantly greater on the rhBMP-2 side compared to the control side at 7 days. Differentiation also occurred all through the early stage (up to 14 days) on the rhBMP-2 side. Therefore, it was demonstrated in this experiment that rhBMP-2 accelerated proliferation of mesenchymal cells and their differentiation into osteoblastic cells, enabling these sockets to heal faster than the controls.

No cartilage formation was detected at any time point studied in this experiment. Rather, direct bone formation (intramembranous bone formation) was observed both inside and outside of the socket. In most experimental studies, chondrogenesis has been observed in the process of new bone formation (endochondral bone formation). Some studies demonstrating direct osteogenesis concluded that differences in culture system (in vitro) or environment of graft sites (in vivo) may be responsible for cartilage induction or non-induction.<sup>25,26</sup> Low concentrations of applied rhBMP-2 may be one reason for the chondrogenesis in rat mandibular bone defects observed by King and associates.<sup>18</sup> However, this experiment had different findings in the rat maxilla, which may

be the result of environmental differences and/or of the different carrier used. Perhaps periodontal ligament fibroblasts and endosteal fibroblastic cells present in the rat maxilla<sup>27</sup> are committed osteoprogenitors; however, this remains unclear.

Poly(lactic acid)/poly(glycolic acid) copolymer alone has been recommended as a useful carrier by many researchers.<sup>28,29</sup> The major part of the carrier used in this experiment contains PLGA. The gelatin sponge, used as a vehicle only, was resorbed quickly 7 days after grafting. Very few unresorbed PLGA polymer particles could be observed at 56 days, and no particles were seen at 84 days in H&E-stained paraffin serial sections on the rhBMP-2 side. Slow, gradual resorption of the polymer may have delayed the healing of socket to some extent. On the other hand, the PLGA may have delivered rhBMP-2 molecules (grafted or endogenous) for a longer period to continue cortical bone formation. All of these reasons support the use of PLGA/GS as an rhBMP-2 carrier.

## SUMMARY

Prognoses for rhBMP-2-induced alveolar ridge preservation after tooth extraction have seldom been reported. In this experiment, fine structural and histomorphologic observation was performed over 84 days in rats. Dome-shaped bone formation induced by rhBMP-2 was seen at the opening of the socket and eventually remodeled to a flat surface that was continuous with the adjoining ridges. Light microscopy and SEM showed that thick cortical bone with a smooth periosteal surface was formed on the rhBMP-2 side. The findings of accelerated alveolar

bone formation by rhBMP-2 and adaptation with the preexisting bone to create cortical alveolar ridge bone in rats suggest that the rhBMP-2 with PLGA/GS carrier may be useful in aiding socket healing.

## ACKNOWLEDGMENT

This investigation was supported by Ministry of Education, Science, Sports and Culture of Japan. The authors would like to offer their gratitude to the late Professor Haruka Kusakari of the Department of Fixed Prosthodontics, Niigata University School of Dentistry, for professional support and advice. The rhBMP-2 and the carrier were kindly provided by Yamanouchi Pharmaceutical Industries, Tokyo, Japan.

## REFERENCES

- Carlsson GE, Persson G. Morphologic changes of the mandible after extraction and wearing of dentures. A longitudinal, clinical, and x-ray cephalometric study covering 5 years. *Odontologisk Rev* 1967;18:27-54.
- Breine U, Brånemark P-I. Reconstruction of alveolar jaw bone. An experimental and clinical study of immediate and preformed autologous bone grafts in combination with osseointegrated implants. *Scand J Plast Reconstr Surg* 1980;14:23-48.
- Urist MR. Bone formation by autoinduction. *Science* 1965;150:893-899.
- Wozney JM, Rosen V, Celeste AJ, et al. Novel regulators of bone formation: Molecular clones and activities. *Science* 1988;242:1528-1534.
- Schenk RK, Buser D, Hardwick WR, Dahlin C. Healing pattern of bone regeneration in membrane-protected defects. A histologic study in the canine mandible. *Int J Oral Maxillofac Implants* 1994;9:13-29.
- Howell TH, Fiorellini J, Jones A, et al. A feasibility study evaluating rhBMP-2/absorbable collagen sponge device for local alveolar ridge preservation or augmentation. *Int J Periodontics Restorative Dent* 1997;17:125-139.
- Rutherford RB, Sampath TK, Rueger DC, Taylor TD. Use of bovine osteogenic protein to promote rapid osseointegration of endosseous dental implants. *Int J Oral Maxillofac Implants* 1992;7:297-301.
- Lindhe A, Hedner E. Recombinant bone morphogenetic protein-2 enhances bone healing, guided by osteopromotive e-PTFE membranes: An experimental study in rats. *Calcif Tissue Int* 1995;56:549-553.
- Cochran DL, Jones AA, Lilly LC, Fiorellini JP, Howell H. Evaluation of recombinant human bone morphogenetic protein-2 in oral applications including the use of endosseous implants: 3-year results of a pilot study in humans. *J Periodontol* 2000;71:1241-1257.
- Alpaslan C, Irie K, Takahashi K, et al. Long-term evaluation of recombinant human bone morphogenetic protein-2 induced bone formation with a biologic and synthetic delivery system. *Br J Oral Maxillofac Surg* 1996;34:414-418.
- Toriumi DM, Kotler HS, Luxenberg DP, Holtrop ME, Wang EA. Mandibular reconstruction with a recombinant bone-inducing factor. *Arch Otolaryngol Head Neck Surg* 1991;117:1101-1112.
- Hoshi K, Amizuka N, Sakou T, Kurokawa T, Ozawa H. Fibroblasts of spinal ligaments pathologically differentiate into chondrocytes induced by human bone morphogenetic protein-2: Morphological examinations for ossification of spinal ligaments. *Bone* 1997;21:155-162.
- Wang EA, Rosen V, D'Alessandro JS, et al. Recombinant human bone morphogenetic protein induces bone formation. (cartilage induction). *Proc Natl Acad Sci* 1990;87:2220-2224.
- Sigurdsson TJ, Tatakis DN, Lee MB, Wikesjo UM. Periodontal regenerative potential of space-providing expanded polytetrafluoroethylene membranes and recombinant human bone morphogenetic proteins. *J Periodont Res* 1995;66:511-521.
- Cook SD, Salkeld SL, Rueger DC. Evaluation of recombinant osteogenic protein-1 (rhOP-1) placed with dental implants in fresh extraction sites. *J Oral Implantol* 1995;21:281-289.
- Reddi AH, Huggins C. Biochemical sequences in the transformation of normal fibroblasts in adolescent rats. *Proc Natl Acad Sci USA* 1972;69:1601-1605.
- Ting K, Petropoulos LA, Iwatsu M, Nishimura I. Altered cartilage phenotype expressed during intramembranous bone formation. *J Bone Miner Res* 1993;8:1377-1386.
- King GN, King N, Cruchley AT, Wozney JM, Hughes FJ. Recombinant human bone morphogenetic protein-2 promotes wound healing in rat periodontal fenestration defects. *J Dent Res* 1997;76:1460-1470.
- Correll JT, Prentice HR, Wise EC. Biologic investigations of a new absorbable sponge. *Surg Gynecol Obstet* 1945;81:585-589.
- Kinoshita A, Oda S, Takahashi K, Yokota S, Ishikawa I. Periodontal regeneration by application of recombinant human bone morphogenetic protein-2 to horizontal circumferential defects created by experimental periodontitis in beagle dogs. *J Periodontol* 1997;68:103-109.
- Grazzner HG. Monoclonal antibody to 5-bromo and 5-iododeoxyuridine: A new reagent for detection of DNA replication. *Science* 1982;218:474-475.
- Chen TL, Bates RL, Dudley A, Hammonds RG Jr, Amento EP. Bone morphogenetic protein-2b stimulation of growth and osteogenic phenotypes in rats osteoblast-like cells: Comparison with TGF- $\beta$ . *J Bone Miner Res* 1991;6:1387-1393.
- Yamaguchi A, Katagiri T, Ikeda T, Wozney JM, Rosen V, Wang EA. Recombinant human bone morphogenetic protein-2 stimulates osteoblastic maturation and inhibits myogenic differentiation in vitro. *J Cell Biol* 1991;113:681-687.
- Stein GS, Lian JB. Molecular mechanisms mediating proliferation/differentiation interrelationships during progressive development of the osteoblast phenotype. *Endocrinol Rev* 1993;14:424-442.
- Iwasaki M, Nakahara H, Nakase T, et al. Bone morphogenetic protein-2 stimulates osteogenesis but does not affect chondrogenesis in osteochondrogenic differentiation of periosteum-derived cells. *J Bone Miner Res* 1991;9:1195-1204.
- Rosen V, Thies RS. The BMP proteins in bone formation and repair. *Trends Genet* 1992;8:97-102.
- Lin WL, McCulloch CAG, Cho MI. Differentiation of periodontal ligament fibroblasts into osteoblasts during socket healing after tooth extraction in the rat. *Anat Rec* 1994;240:492-509.
- Hollinger JO, Battistone GC. Biodegradable bone repair materials. Synthetic polymers and ceramics. *Clin Orthop Rel Res* 1986;207:209-305.
- Baum BJ, Mooney DJ. The impact of tissue engineering on dentistry. *J Am Dent Assoc* 2000;131:309-318.